Journal of Solid State Chemistry **149,** 341–348 (2000)
doi:10.1006/jssc.1999.8538, available online at http://www.idealibrary.com on IDEAL®

Bi–La-Based Oxide Conductors with Rhombohedral Bi–Sr–O Type: Structural and Conductivity Properties Optimization by Polycationic Substitutions for La

M. Drache,[1] J. P. Wignacourt, and P. Conflant

Laboratoire de Cristallochimie et Physicochimie du Solide, URA CNRS 452, ENSCL et USTL, B.P. 108, 59652 Villeneuve d'Ascq Cedex, France

Received May 25, 1999; in revised form October 7, 1999; accepted October 22, 1999

In $Bi_{0.775}La_{0.225}O_{1.5}$, the best oxide conductor of the hexagonal-layered materials family known as the Bi–Sr–O type, partial polycationic substitutions for La^{3+}, such as $(Ce^{4+}+M_{II}^{2+})$ for 2 La^{3+} (M_{II} = Ba, Pb) or $(M_{VI}^{6+}+3M_{II}^{2+})$ for 4 La^{3+} (M_{VI} = Mo, W; M_{II} = Ba, Pb), have been realized; these substitutions have induced an enlargement of the cationic slab thickness and thus allowed improvement of the conductivity. The resulting modifications of *a* and *c* lattice constants have been interpreted on the basis of the characteristics of the substituting elements (cationic radii and symmetries) and were correlated to the observed conductivity modifications. © 2000 Academic Press

***Key Words*: rhombohedral Bi–Sr–O-type materials; bismuth–lanthanum–based mixed oxides; ionic radius; electronic lone pair; oxide conductors; layered structure–conductivity correlations.**

INTRODUCTION

A recent investigation of structural and conductivity properties of $Bi_{0.775}Ln_{0.225}O_{1.5}$ oxide conductors (Ln = La, Pr, Nd, Sm, Eu, Gd, Tb, Dy), which belong to the dimorphic rhombohedral Bi–Sr–O structural-type family, has proved a close conductivity–composition dependence (1). This has been interpreted on the basis of structural data obtained from Rietveld structure refinements based on previous crystal structure investigations (2–10). The structures are built from cationic slabs parallel to (001) faces of the hexagonal cells. There are 9 formula units of $Bi_{0.775}Ln_{0.225}O_{1.5}$ per hexagonal cell, distributed over 3 slabs. Each slab is constituted from a mixed Bi^{3+}/Ln^{3+} layer, sandwiched between two Bi^{3+} layers, and two oxygen sites are located inside; complementary oxide ions, implied by the formulation stoichiometries, are distributed over one or two sites of the interslab space and exhibit a high mobility, mainly responsible for the conductivity (4). A schematic slab stacking in the hexagonal cell is presented in Fig. 1.

Depending on the rare earth nature, a β_1 high-temperature form is observed, with a closely hexagonal-related structure; its formation from the β_2 low-temperature variety occurs during a phase transition which has been attributed to a cationic disordering in the mixed Bi^{3+}/Ln^{3+} layers; it is accompanied by sudden increases of both lattice parameters, of oxide occupancy in interslab spaces, and of the conductivity. The pure oxide conductor character of the β_1 variety which was clearly demonstrated for the alkaline earth-based solid solutions (4) can also be attributed to lanthanide-based solid solutions (14).

The thickness of the cationic slabs, which is the largest for the lanthanum term (the best oxide conductor ever evidenced in this family: $\sigma_{400°C} = 10^{-3}\,S\,cm^{-1}$ with E_a = 0.8 eV), appears to be the most important factor for these attractive conductivity properties. The larger the slab thickness, the weaker the bonding effects with the conducting oxide ions of interslab spaces, therefore resulting in a high-conductivity level (1). However, the favorable effect of a large slab thickness can be counterbalanced by a decrease of the number of oxide-conducting moities, which is directly related to the number of O^{2-} anions per formulae unit: for example, $Bi_{0.844}Ba_{0.156}O_{1.422}$ which exhibits slab thickness of 6.339 Å (4), larger than $Bi_{0.775}La_{0.225}O_{1.5}$ (6.017 Å), has poorer anionic conductivity performances.

Aiming at improving the conductivity performances of this family, we tried to increase the slab thickness by increasing the average size of cations in the mixed layers by such substitutions that any decrease of the number of counterbalancing oxide ions would be avoided. The resulting modifications of the *a* and *c* lattice constants were interpreted on the basis of the size characteristics of the selected elements. An anisotropic effect of the lone pair, for Pb^{2+} and Bi^{3+}, was also considered. Finally, we tried to correlate these evolutions to the observed conductivity modifications.

[1] To whom correspondence should be addressed. Fax: (33)320436814. E-mail: drache@ensc-lille.fr.

0022-4596/00 $35.00

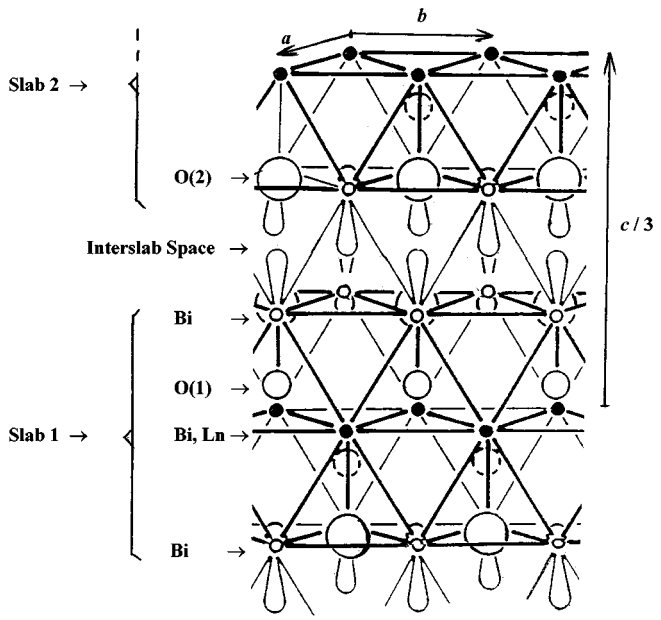

FIG. 1. Representation of slab stacking in the hexagonal cell of Bi–Ln-based oxides.

EXPERIMENTAL

Bismuth–lanthanum-based oxide powder samples were prepared by solid state reaction of mixtures of Bi_2O_3, La_2O_3, and depending on the targeted compositions, reactants based on two other cations in proportions required to finally obtain the molar fraction (oxygen/Σ(metals)) = 1.5. When one of these reactants was PbO or $BaCO_3$, the other had to be a metal oxide with an oxidation number higher than 3: CeO_2, WO_3, or MoO_3. The reactants were prefired overnight at 700°C (La_2O_3, CeO_2), 600°C (Bi_2O_3 and PbO), 400°C (MoO_3), 300°C (WO_3), and 150°C $BaCO_3$), to prevent any trace of hydrate or carbonate. The selection of the synthesized compositions is justified in the Results and Discussion section; stoichiometric proportions corresponding to these compositions were accurately weighted and thoroughly ground in an agate mortar. Each mixture was heated for several 15-h treatments and air-quenched; each thermal treatment was followed by regrinding. Heating temperatures and the number of thermal treatments were determined to obtain the largest composition domains of the pure hexagonal phase, at room temperature, characterized by X-ray diffractometry using a Guinier de Wolff camera (Cu$K\alpha$ radiation). Two successive treatments at 700 and 800°C were used for samples with La/Bi ≤ 0.225; for samples with $0.225 < (\text{La/Bi}) < 0.375$, 3–5 thermal treatments, and a final heating temperature ranging between 850 and 975°C, were necessary. All samples were then annealed at 620°C for 3–7 days of treatments.

Powder diffraction data were obtained on a Siemens D5000 diffractometer using a Bragg Brentano geometry, with a back-monochromatized Cu$K\alpha$ radiation. Diffraction spectra were scanned by steps of 0.02° (2θ) over the angle range 15°–80°, with a counting time of 1.5 s per step. Each sample was rotated at 3.14 rad s^{-1} during the data recording, to minimize the orientation effects resulting from the material compaction. The positions of the peaks were determined by means of the software package DIFFRACT-AT from SOCABIM. The accurate cell parameters of the different samples were refined from 20 to 30 reflections. (hexagonal setting).

Conductivity properties of materials with molar fraction (bismuth/Σ(metals)) = 0.775 were investigated. Powder samples were pelletized at room temperature (diameter, 5 mm; thickness, ca. 3 mm) and then sintered at 800° C for 15–60 h of thermal treatments, and finally annealed at 620°C for 60 h. Compaction was in all cases ranging between 0.90 and 0.95. Gold electrodes were vacuum deposited on both flat surfaces of pellets using the sputtering method. The measurements were performed by impedance spectrometry in the frequency range 1–10^6 Hz, using a frequency response analyzer Schlumberger 1170; for each investigated temperature a set of values was recorded after a 1 h of stabilization time. The results were interpreted from $\log \sigma = f(1000/T)$ Arrhenius plots.

RESULTS AND DISCUSSION

To expand the slab thickness in the $Bi_{0.775}La_{0.225}O_{1.5}$-layered structure, by lanthanum substitution, we selected various combinations of stable ion pairs with a mean oxidation number of +3 and an average size larger than that of the La^{3+} ions (11, 12). Among the different possibilities, we avoided the alkaline metals because of their well-known moisture sensitivity; we selected pseudoions $(aA + bB)^{3+}$ (ion combinations of elements A and B with respectively molar fractions a and b) such as $\frac{1}{4}Mo^{6+} + \frac{3}{4}Ba^{2+}$, $\frac{1}{4}W^{6+} + \frac{3}{4}Ba^{2+}$, $\frac{1}{2}Ce^{2+} + \frac{1}{2}Ba^{2+}$, which exhibited average ionic radii (hexacoordination) of respectively 1.17, 1.165, and 1.08 Å, values higher than the corresponding La^{3+} radius (1.061 Å).

Aiming at evaluating the sterical effect of the $6s^2$ electronic lone pair of bismuth belonging to the sandwiched cationic layers, we investigated materials with various occupancy ratios of the site of this anisotropic element in these layers, and therefore for molar fractions (bismuth/Σ(metals)) in materials varying in a range including 0.775. Starting from the model-phase $Bi_{0.775}La_{0.225}O_{1.5}$, we synthesized $Bi_{1-y}La_yO_{1.5}$ mixed oxides in a large composition range.

Taking into account the isoelectronic character of Bi^{3+} and Pb^{2+} cations, materials with molar fraction (bismuth/Σ(metals)) = 0.775 and various Pb^{2+} concentrations were also examined: $Bi_{0.775}La_{0.225(1-x)}W_{(0.225/4)x}Pb_{(0.225\times 3/4)x}$

TABLE 1
Characteristics of Synthesized $Bi_{0.775}La_{0.225}O_{1.5}$-Related Solid Solutions

$aA + bB$[a]	$r_{VI\,mean}$ (Å)[b]	Formulae	Composition ranges[c] maxima steps: 0.1 for x, 0.025 for y
$\frac{1}{4}Mo + \frac{3}{4}Ba$	1.17	$Bi_{0.775}La_{0.225(1-x)}Mo_{(0.225/4)x}Ba_{(0.225\times3/4)x}O_{1.5}$	$0 \le x \le 0.3$
$\frac{1}{4}W + \frac{3}{4}Ba$	1.165	$Bi_{0.775}La_{0.225(1-x)}W_{(0.225/4)x}Ba_{(0.225\times3/4)x}O_{1.5}$	$0 \le x \le 0.3$
$\frac{1}{2}Ce + \frac{1}{2}Ba$	1.08	$Bi_{0.775}La_{0.225(1-x)}Ce_{(0.225/2)x}Ba_{(0.225/2)x}O_{1.5}$	$0 \le x \le 0.3$
La	1.061	$Bi_{0.775}La_{0.225}O_{1.5}$	
$\frac{1}{4}Mo + \frac{3}{4}Pb$	1.035	$Bi_{0.775}La_{0.225(1-x)}Mo_{(0.225/4)x}Pb_{(0.225\times3/4)x}O_{1.5}$	$0 \le x \le 0.3$
$\frac{1}{4}W + \frac{3}{4}Pb$	1.03	$Bi_{0.775}La_{0.225(1-x)}W_{(0.225/4)x}Pb_{(0.225\times3/4)x}O_{1.5}$	$0 \le x \le 0.3$
Bi	1.02	$Bi_{1-y}La_yO_{1.5}$	$0.15 \le y \le 0.375$
$\frac{1}{2}Ce + \frac{1}{2}Pb$	0.99	$Bi_{0.775}La_{0.225(1-x)}Ce_{(0.225/2)x}Pb_{(0.225/2)x}O_{1.5}$	$0 \le x \le 0.3$

[a] Pseudosubstituents for lanthanum.
[b] $r_{VI\,mean}$ corresponds to the average radius of the corresponding (A, B) cation(s) of the first column and is calculated using data from Refs. (11, 12).
[c] Investigated composition domains.

$O_{1.5}$ and $Bi_{0.775}La_{0.225(1-x)}Ce_{(0.225/2)x}Pb_{(0.225/2)x}O_{1.5}$, although in these solid solutions, the averaged ionic radii of $(aA + bB)^{3+}$ pseudoions are smaller than those of La^{3+}.

For samples with fixed molar fraction (bismuth/Σ(metals)) = 0.775, substitution ratios (x) for lanthanum were varied with an x step of 0.1. In all cases the composition range $0 \le x \le 0.3$ revealed a pure hexagonal-layered phase, whereas the samples prepared for $x \ge 0.3$ were polyphasic mixtures. The precise determination of single-phase domains was not undertaken. The $Bi_{1-y}La_yO_{1.5}$ mixed oxide materials were first synthesized by a y step of 0.025 for the composition range $0.15 \le y \le 0.30$. Thus, the composition–cell parameters dependence revealed the existence of anomalies which could indicate an ordering of the mixed cations. Synthesis was then realized for $0.30 < y \le 0.375$ and two samples were also prepared for y values corresponding to a potential ordering of 3 Bi and 4 La, 1 Bi and 6 La of the slab-sandwiched layers within a bidimensional supercell of 7 hexagonal cells respectively:

$$4_{(La)}/((4_{(La)} + 3_{(Bi)}) + 7_{(Bi)} + 7_{(Bi)})) = 0.190 \quad \text{and}$$

$$6_{(La)}/((6_{(La)} + 1_{(Bi)}) + 7_{(Bi)} + 7_{(Bi)})) = 0.286.$$

Table 1 lists the selected $(aA + bB)^{3+}$ pseudoions with their averaged ionic radii (hexacoordination) altogether with the general formulae and the composition ranges of the synthesized materials corresponding to the pure hexagonal-layered phases). The evolutions of the refined lattice parameters versus composition (Table 2) characterize the existence of various solid solutions.

Taking into account the Bi–Sr–O rhombohedral-type structural model built from cationic slabs, each slab, corresponding to 1/3 of a tridimensional hexagonal cell, contains 3 cations; it is now constituted with $2Bi^{3+}$ layers sandwiching an intermediate layer either of (Bi^{3+}, La^{3+}, and $(aA + bB)^{3+}$) or (Bi^{3+}, La^{3+}) for $Bi_{1-y}La_yO_{1.5}$ mixed oxides ($y < 0.333$). The cationic mean radius in this mixed layer was calculated using the ionic radii data known for 6-fold coordination (11, 12): $r_{mean} = ((0.775 \times 3) - 2)r_{Bi} + 0.225 \times 3(1 - x)r_{La} + 0.225 \times 3x(ar_A + br_B)$ when $x(aA + bB)^{3+}$ substitutes for xLa^{3+} in $Bi_{0.775}La_{0.225}O_{1.5}$; $r_{mean} = (((1 - y) \times 3) - 2)r_{Bi} + 3yr_{La}$, for $Bi_{1-y}La_yO_{1.5}$ samples. Figure 2 evidences, for each $(aA + bB)$ pseudosubstituent, a linear relationship between the hexagonal cell volume and the mean cationic radius. This mean radius appears to be a good investigation parameter of structure–composition correlations in these materials: we observe a cell volume contraction for the pseudosubstituents smaller than lanthanum, whereas an expansion occurs for the largest substituents.

Figure 3 presents the lattice constants evolutions versus the mean cationic radius of elements in the mixed sheet for

TABLE 2
Lattice Parameters (Å) of a Hexagonal Cell for the Various Synthesized $Bi_{0.775}La_{0.225}O_{1.5}$-Related Solid Solutions

A/B	x	a	c	y	a	c
Mo/Ba	0.1	4.027(1)	27.792(7)	0.15	4.000(1)	27.884(8)
Mo/Ba	0.2	4.032(2)	27.933(9)	0.175	4.011(1)	27.785(8)
Mo/Ba	0.3	4.034(2)	28.02(2)	0.190	4.0148(5)	27.702(5)
W/Ba	0.1	4.028(2)	27.76(2)	0.2	4.018(1)	27.676(8)
W/Ba	0.2	4.027(2)	27.87(1)	0.225	4.023(1)	27.618(6)
W/Ba	0.3	4.029(1)	27.98(2)	0.25	4.029(1)	27.572(6)
Ce/Ba	0.1	4.018(2)	27.764(6)	0.275	4.0350(6)	27.514(4)
Ce/Ba	0.2	4.018(1)	27.857(9)	0.286	4.035(1)	27.488(5)
Ce/Ba	0.3	4.016(2)	27.93(2)	0.3	4.037(1)	27.491(7)
W/Pb	0.1	4.015(1)	27.73(1)	0.317	4.039(1)	27.465(4)
W/Pb	0.2	4.002(1)	27.866(8)	0.35	4.0419(7)	27.478(5)
W/Pb	0.3	3.993(2)	27.97(1)	0.375	4.0424(9)	27.516(12)

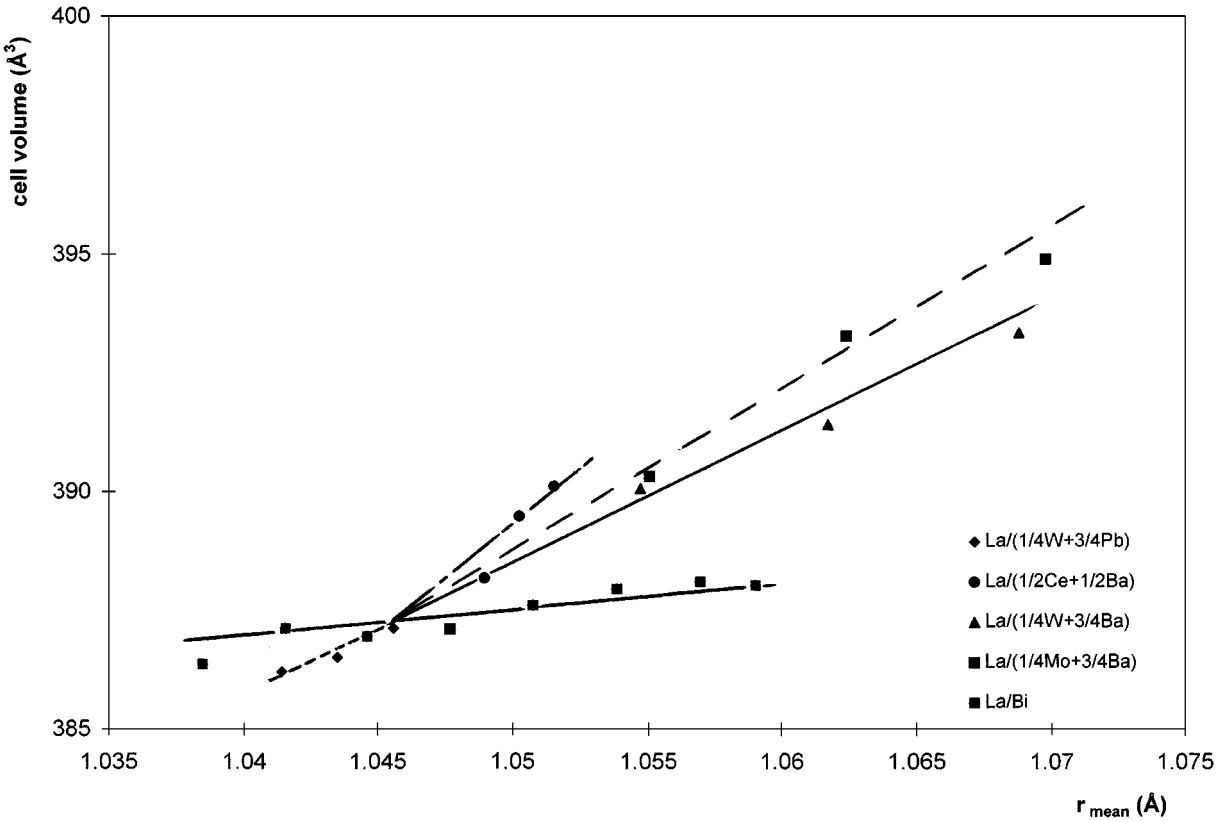

FIG. 2. $Bi_{0.775}La_{0.225}O_{1.5}$-related solid solutions: evolution of hexagonal cell volume versus mean radius of mixed cations.

samples of $Bi_{0.775}La_{0.225(1-x)}W_{(0.225/4)x}Pb_{(0.225\times 3/4)x}O_{1.5}$ and $Bi_{0.775}La_{0.225(1-x)}Mo_{(0.225/4)x}Ba_{(0.225\times 3/4)x}O_{1.5}$. In this last solid solution, resulting from the substitution of La^{3+} by a larger pseudoion (a combination of two spherical ions) statistically occupying the mixed cationic sites, an increase of both the *a* and *c* lattice constants occurs, leading to an expansion of the cell volume. For the other case ($Bi_{0.775}La_{0.225(1-x)}W_{(0.225/4)x}Pb_{(0.225\times 3/4)x}O_{1.5}$ solid solution), the substituent exhibits an average radius smaller than lanthanum, and the substitution induces a decrease of *a*, but an increase of the *c* parameter. This behavior can be interpreted on the basis of different considerations: Pb^{2+} as well as Bi^{3+} ions exhibit an anisotropic symmetry. As has been evidenced in $Bi_{0.7}La_{0.3}O_{1.5}$ structure determination (6), bismuth electronic lone pairs, whatever the cationic sheets (external of sandwiched sheets of the slabs), are oriented in the *c*-axis direction of the hexagonal cell. During partial replacement of spherical La^{3+} by $(\frac{1}{4}W^{6+} + \frac{3}{4}Pb^{2+})$, lone pairs of introduced Pb^{2+} cations are likely to take the *c*-axis direction, similar to the bismuth electronic lone pairs; this anisotropical effect yields an increase of the slab thickness and therefore of the *c*-lattice parameter, whereas *a* decreases (radius$_{VI}$ $La^{3+} = 1.061$ Å; radius$_{VI}$ $Pb^{2+} = 1.18$ Å).

A similar anisotropic effect is evidenced by the composition versus cell parameters dependence of $Bi_{1-y}La_yO_{1.5}$ mixed oxides, displayed in Fig. 4. So, Bi^{3+} substitution for La^{3+} going from $Bi_{0.666}La_{0.333}O_{1.5}$ to $Bi_{0.775}La_{0.225}O_{1.5}$ and then to $Bi_{0.85}La_{0.15}O_{1.5}$ leads to a decrease of the cell volume (in agreement with the constituents size modification: radius$_{VI}$ $Bi^{3+} = 1.02$ Å), corresponding to a decrease of *a* , but an increase of the *c* lattice constant. This confirms the orientation of the Bi^{3+} electronic lone pair along the *c*-axis and indicates that the Bi^{3+} ion (hexacoordinated) exhibits a real dimension larger than the La^{3+} radius$_{VI}$ in the electronic lone pair direction, and therefore an effective radius smaller than the standard value$_{VI}$ 1.02 Å announced for this element (11, 12) in the (*a*, *b*) perpendicular plane. It was observed in a previous investigation of the $Bi_{1-y}Sm_yO_{1.5}$ analogous solid solution (13) with the increase of both cell parameters during bismuth for samarium substitution. The effective radius$_{VI}$, in the plane perpendicular to the Bi^{3+} lone pair direction, appears therefore to be larger than the Sm^{3+} radius$_{VI}$ (0.964 Å).

Careful examination of Fig. 4 evidences different linear evolution domains with breaking points identified for *y* values $\cong 0.18, 0.275$ and 0.333. This last ratio corresponds

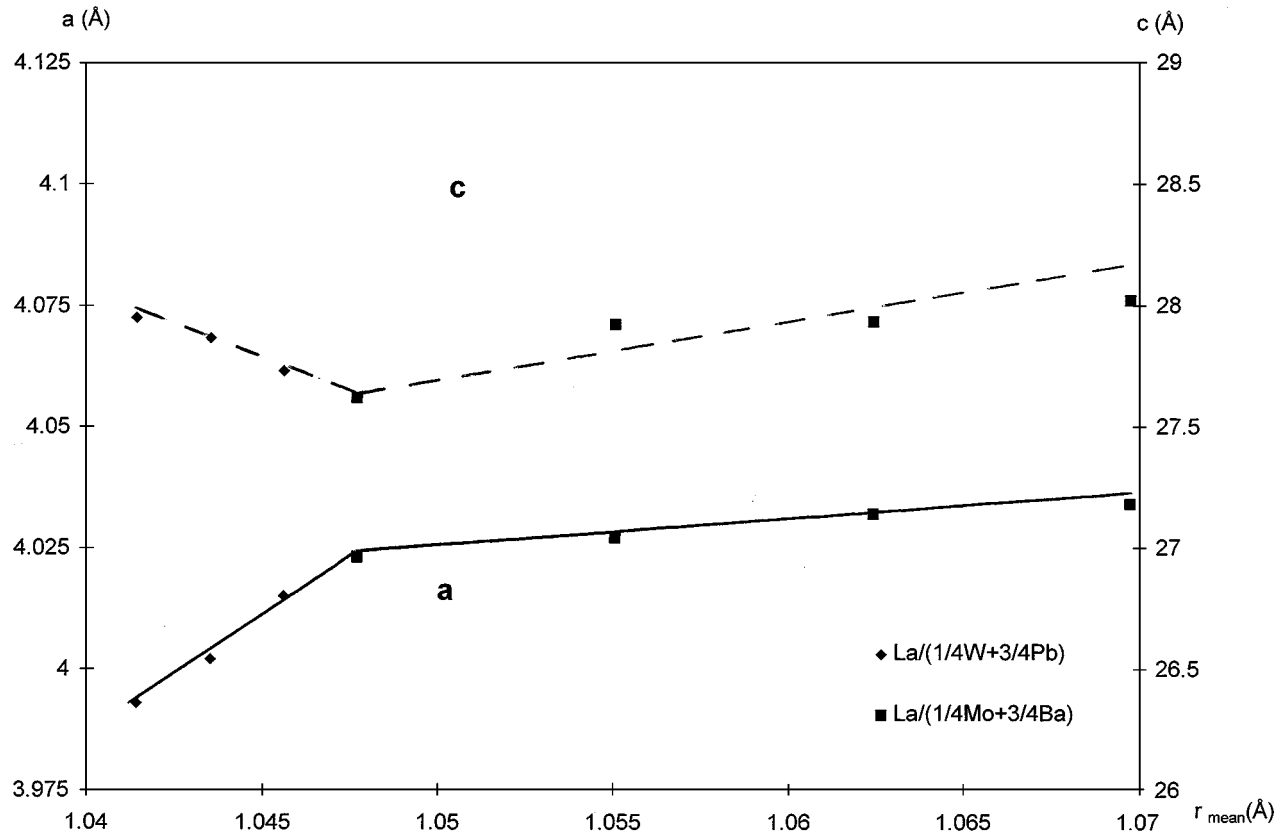

FIG. 3. Evolution of lattice parameters versus mean radius of mixed cations for materials $Bi_{0.775}La_{0.225(1-x)}W_{(0.225/4)x}Pb_{(0.225\times3/4)x}O_{1.5}$ and $Bi_{0.775}La_{0.225(1-x)}Mo_{(0.225/4)x}Ba_{(0.225\times3/4)x}O_{1.5}$.

to the particular layered model, where sandwiched cationic layers are only occupied by lanthanum; the two other compositions are likely to correspond to the hypothetic cationic ordered phases predicted from our previous investigation (1).

Among the different solid solutions with constant bismuth molar concentrations, $Bi_{0.775}La_{0.225(1-x)}Mo_{(0.225/4)x}Ba_{(0.225\times3/4)x}O_{1.5}$ and $Bi_{0.775}La_{0.225(1-x)}W_{(0.225/4)x}Pb_{(0.225\times3/4)x}O_{1.5}$ lead to the largest c lattice constant values and respectively to nearly the largest and the smallest a lattice constant value. They both appear well adapted for an investigation of their conductivity properties, aiming at the identification of a correlation with their structural features.

In the $Bi_{1-y}La_yO_{1.5}$ solid solution, the cell parameters modification which occurs during the bismuth content increase is similar but less significant than that of $Bi_{0.775}La_{0.225(1-x)}W_{(0.225/4)x}Pb_{(0.225\times3/4)x}O_{1.5}$; thus, the bismuth-richest samples ($y \leq 0.225$) could present a slightly higher anionic conductivity than $Bi_{0.775}La_{0.225}O_{1.5}$ mixed oxide, resulting from lattice constant modification. Two other features influence the conductivity level of the samples: the polarizability of the cationic sublattice, which increases with the Bi^{3+} content, induces a favorable effect, whereas the probable ordering in the cationic mixed layer for the bismuth-richest samples is an inhibiting factor for the anionic O^{2-} mobility. An investigation of the conductivity properties of this solid solution, which requires an examination of a significant series of compositions, will be reported in a future paper dealing with the ordered structure determination.

Conductivity measurements were performed during heating–cooling runs between 300 and 600°C and then between 300 and 780°C. The results corresponding to the initial heating treatments cannot be used because of the evolution of the gold electrode–material interface during the corresponding run. Measurements realized for subsequent treatments lead to Arrhenius plots constituted by a single linear domain for the first cooling run and two linear domains for the following runs; for each temperature, a good reproducibility of conductivity values is observed from one run to another; in the intermediate area (525–650°C, depending on the material), which characterizes the well-known $\beta_2 \leftrightarrow \beta_1$ transition by a faster conductivity evolution, σ_{cooling} is higher than σ_{heating}. Arrhenius plots corresponding to measurements performed during cooling runs are presented for

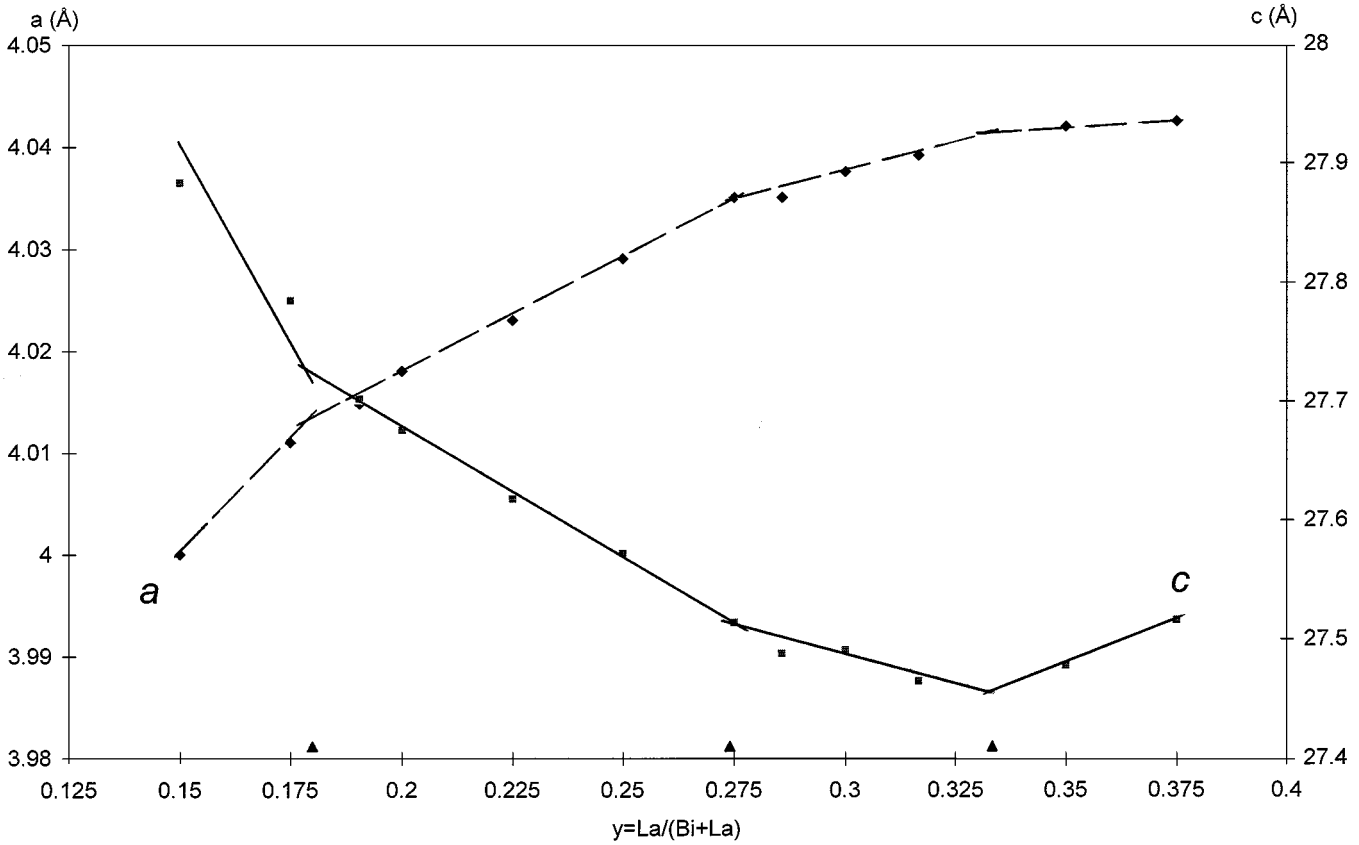

FIG. 4. Composition dependence of cell parameters for $Bi_{1-y}La_yO_{1.5}$ solid solution.

$Bi_{0.775}La_{0.225(1-x)}Mo_{(0.225/4)x}Ba_{(0.225\times 3/4)x}O_{1.5}$ (Fig. 5a) and for $Bi_{0.775}La_{0.225(1-x)}W_{(0.225/4)x}Pb_{(0.225\times 3/4)x}O_{1.5}$ Fig 5b), with $x = 0$, 0.1, 0.2, and 0.3.

The considered solid solutions exhibit two opposite variations of their isothermal conductivity behaviors versus x. For the Mo–Ba containing solid solution, σ increases during x variation from 0 to 0.1 and then decreases to values lower than the initial value for $x = 0.2$ and 0.3; for the W–Pb containing solid solution, σ decreases during x variation from 0 to 0.2 and then increases to a value higher than that of the initial term ($x = 0$). The Arrhenius plots which correspond to the best conductors of both solid solutions, in temperature ranging either under 525°C or over 650°C, are quite similar and interesting: $\sigma_{400°C} \cong 1.4 \times 10^{-3}\,S\,cm^{-1}$.

Although the variations of the conductivity linked to the lanthanum substitutions appear to be small, the observed conductivity evolutions, with extreme σ values, related to the x variation, seem to imply the occurrence of two antgonistic influences.

The cell parameters evolution is unambiguously favorable during the Mo–Ba for La substitutions ($a\uparrow$ and $c\uparrow$). W + Pb for La substitution induces a decrease of a, thus inhibiting the motion of O^{2-} ions from the slab to the interslab space; in the same time, the increase of c results essentially from an increase of the slab thickness, which was characterized as a favorable factor to the O^{2-} mobility in the interslab space.

On the basis of known ionic radii (11, 12) we determined the evolutions of structure compacity (ions volume/cell volume) corresponding to the substitutions for lanthanum. The decrease observed for Mo + Ba for La substitution inclusively appears beneficial to the oxide mobility, whereas the increase which occurs for W + Pb for La substitution seems to have a negative effect. However, it is necessary to discern the variations of each ionic compacity (ions volume for a given element/cell volume), knowing the high polarizability of Bi^{3+} or Pb^{2+} ions, beneficial for the oxide conductivity, and the large electropositive character of Ba^{2+} ions which inhibits the corresponding conductivity σ. For the first substitution type, the overall decrease of the structure compacity also corresponds to the decrease of Bi^{3+} compacity and the increase of the Ba^{2+} related one, these two evolutions inhibiting the conductivity performances; for the second substitution type, the increase of the structural compacity corresponds to the increases of Bi^{3+} and Pb^{2+} compacities, both variations favoring σ. On the basis of this

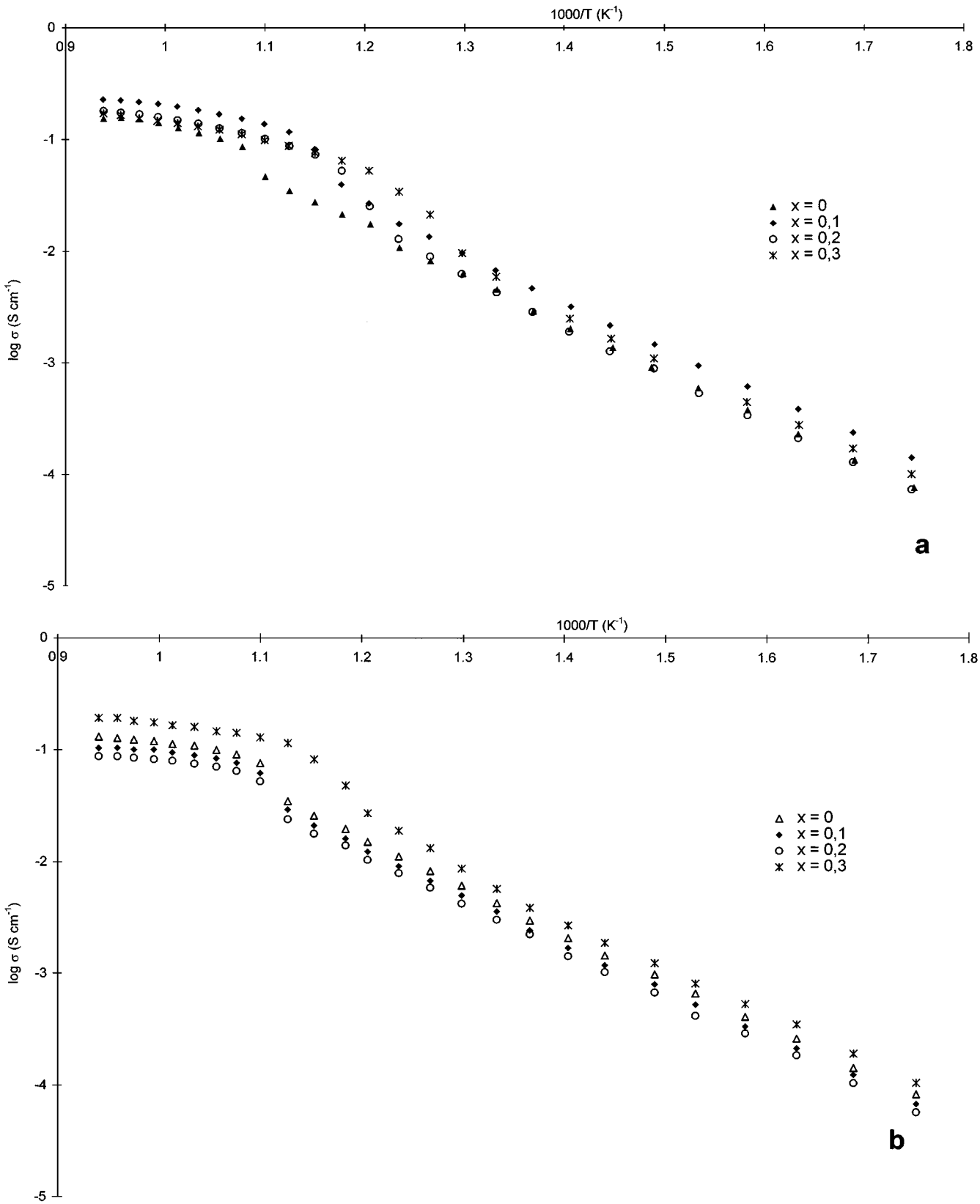

FIG. 5. (a and b) Arrhenius plots upon cooling runs of mixed cations ($\frac{1}{4}$Mo + $\frac{3}{4}$Ba) (a) or ($\frac{1}{4}$W + $\frac{3}{4}$Pb) (b) for lanthanum substitution in $Bi_{0.775}La_{0.225}O_{1.5}$ material.

discussion, the observed $\sigma = f(x)$ evolutions seem to indicate that, during lanthanum substitution, the structural modification exhibits an influence only for low substitution ratios, whereas the modification of the polarizability effect of the cations sublattice is mostly effective for larger substitution ratios.

CONCLUSION

Cationic substitutions in $Bi_{0.775}La_{0.225}O_{1.5}$ mixed oxides, with a Bi–Sr–O rhombohedral structural type, were chosen to maintain a constant oxide number. These substitutions proved direct correlations between the lattice parameters evolution of the β_2 hexagonal cell and selected modifications in the samples formulae; these correlations can be explained on the basis of the structural features (structures built of cationic slabs composed of two Bi layers sandwiching one mixed Bi/M layer, with the orientation of the bismuth electronic lone pairs along the *c*-axis direction, perpendicular, to the slabs). We observe a relationship between the average cation ionic radius within the sandwiched cationic layers and the unit cell volume; the cell parameters evolution corresponding to the volume modification depends on the size difference of lanthanum and substituting mixed ions. For the biggest mixed substituents ((Mo or W) + Ba), the increase of volume corresponds to an increase of both the *a* and *c* cell parameters; when the size difference is small ((Ce + Ba) or (W + Pb) for La substitutions), a slight decrease of *a* and an increase of the *c* parameter occur, corresponding respectively to an increase (Ce + Ba) or a decrease (W + Pb) of the cell volume. This behavior, which is also observed when bismuth substitutes for lanthanum, is justified by the orientation in the *c*-axis direction of Bi^{3+} and Pb^{2+} electronic lone pairs. The evolution of isothermal conductivity of these materials, during lanthanum substitution, are very small. They result essentially not only from the modification of the slab thickness, which varies nearly as the *c* lattice constant but also from interactions between the cations and the oxide ions of the interslabs space: the presence of Ba^{2+} inhibits the O^{2-} mobility, whereas Bi^{3+} or Pb^{2+} favors it.

ACKNOWLEDGMENTS

The authors are very grateful to Mrs. Nora Bouremma-Djelal and Mrs. Laurence Burylo-Dhuime for their help with samples syntheses and collection of powder X-ray diffraction data.

REFERENCES

1. M. Drache, S. Obbade, J. P. Wignacourt, and P. Conflant, *J. Solid State Chem.* **142,** 349 (1999).
2. P. Conflant, J. C. Boivin, G. Nowogrocki, and D. Thomas, *Solid State Ionics* **9/10,** 925 (1983).
3. P. Conflant, J. C. Boivin, and D. Thomas, *J. Solid State Chem.* **35,** 192 (1980).
4. P. Conflant, Thesis, University of Lille, 1985.
5. M. Drache, J. P. Wignacourt, and P. Conflant, *Solid State Ionics* **86–88,** 289 (1996).
6. D. Mercurio, M. El Farissi, J. C. Champarneaud-Mesjard, B. Frit, and P. Conflant, *J. Solid State Chem.* **80,** 133 (1989).
7. D. Mercurio, J. C. Champarneaud-Mesjard, B. Frit, P. Conflant, J. C. Boivin, and J. B. Vogt, *J. Solid State Chem.* **112,** 1 (1994).
8. S. K. Blower and C. Greaves, *Mater. Res. Bull.* **23,** 765 (1988).
9. R. J. D. Tilley, *J. Solid State Chem.* **41,** 233 (1982).
10. R. L. Withers, and H. Rossell, *J. Solid State Chem.* **118,** 66 (1995).
11. R. D. Shannon and C. T. Prewitt, *Acta Crystallogr. B* **26,** 1046 (1970).
12. R. D. Shannon, *Acta Crystallogr. A* **32,** 751 (1976).
13. P. Conflant, C. Follet-Houttemane, and M. Drache, *J. Mater. Chem.* **1,** 649 (1991).
14. P. Conflant and M. Drache, unpublished results.